

Electronic Supplementary Information

**A benzoxazole derivative as an inhibitor of anaerobic choline metabolism by human gut microbiota**

Moustafa T. Gabr,<sup>a\*</sup> David Machalz,<sup>b</sup> Szymon Pach,<sup>b</sup> and Gerhard Wolber<sup>b</sup>

<sup>a</sup>Department of Radiology, Stanford University School of Medicine, Stanford, CA, 94305. Email: gabr2003@gmail.com

<sup>b</sup>Freie Universitaet Berlin, Institute of Pharmacy, Pharmaceutical and Medicinal Chemistry (Computer-Aided Drug Design), Berlin, Germany.

**Contents**

Percentage intact compound remaining of compounds <b>4-18</b> upon incubation with intestinal S9 fraction for 2 hours as determined by LC-MS/MS	S2
Summary of the interactions of the 2 docked poses of BO-I with CutC based on MD simulations	S3
The effect of BO-I (50 $\mu$ M) on choline uptake in <i>Escherichia coli</i> ( <i>E. coli</i> ) MS 200-1 at various added concentrations of <i>d</i> <sub>9</sub> -choline	S4
Evaluation of alcohol dehydrogenase activity using alcohol dehydrogenase activity kit (ab102533) in the absence and presence of different concentrations of BO-I	S4
SPR binding curve for BO-I to CutC	S5
SPR binding curve for BO-I to CutD	S5
Michaelis–Menten plot of the reaction velocity against various concentrations of choline in the absence and presence of BO-I (5 $\mu$ M)	S6
Bacterial growth kinetics based on absorbance measurements in the absence and presence of BO-I (25 $\mu$ M) for (A) <i>E. coli</i> MS 200-1 (B) <i>Klebsiella sp.</i> MS 92-3 (C) <i>Proteus mirabilis</i> , and (D) <i>Clostridium sporogenes</i>	S6
Suggested substrate entry funnel of CutC from <i>D. desulfuricans</i> and <i>K.pneumoniae</i> .	S7
Suggested binding mode of BO-I to the substrate entry funnel of CutC from <i>K. pneumoniae</i>	S8
References	S9

**Table S1.** Percentage intact compound remaining of compounds **4-18** upon incubation with intestinal S9 fraction for 2 hours as determined by LC-MS/MS.

<b>Comp.</b>	<b>% intact compound ± S.D.<sup>a</sup></b>
<b>4</b>	96.4 ± 1.2
<b>5</b>	91.5 ± 3.2
<b>6</b>	90.9 ± 2.5
<b>7</b>	98.6 ± 1.5
<b>8</b>	90.2 ± 1.8
<b>9</b>	95.1 ± 1.4
<b>10</b>	97.1 ± 0.9
<b>11</b>	92.2 ± 2.8
<b>12</b>	93.8 ± 1.7
<b>13</b>	91.1 ± 3.1
<b>14</b>	94.3 ± 1.6
<b>15</b>	93.4 ± 2.5
<b>16</b>	97.2 ± 1.4
<b>17</b>	98.7 ± 0.5
<b>18</b>	96.9 ± 2.1

<sup>a</sup>All experiments were performed in triplicates

**Table S2.** Summary of the interactions of the 2 docked poses of BO-I with CutC based on MD simulations.

Interaction type	Moiety of BO-I	Interacting residue in MD simulations of		Interaction Frequencies [%] for	
		Pose 1	Pose 2	Pose 1	Pose 2
Aromatic	Benzene or Isoxazole Ring	Phe202, Phe388,	Tyr189, Arg141	12	13
	Benzene Ring	Phe202, Phe388, Leu709	Tyr189, Trp195, Ala210, Val211	88	97
Hydrophobic	Cyclopropyl Rest	Tyr189, Trp195, Val211, Phe706	Phe202	87	16
	Piperidinium Ion	Phe202, Asp205, Phe388	Glu186, Asp205	85	64

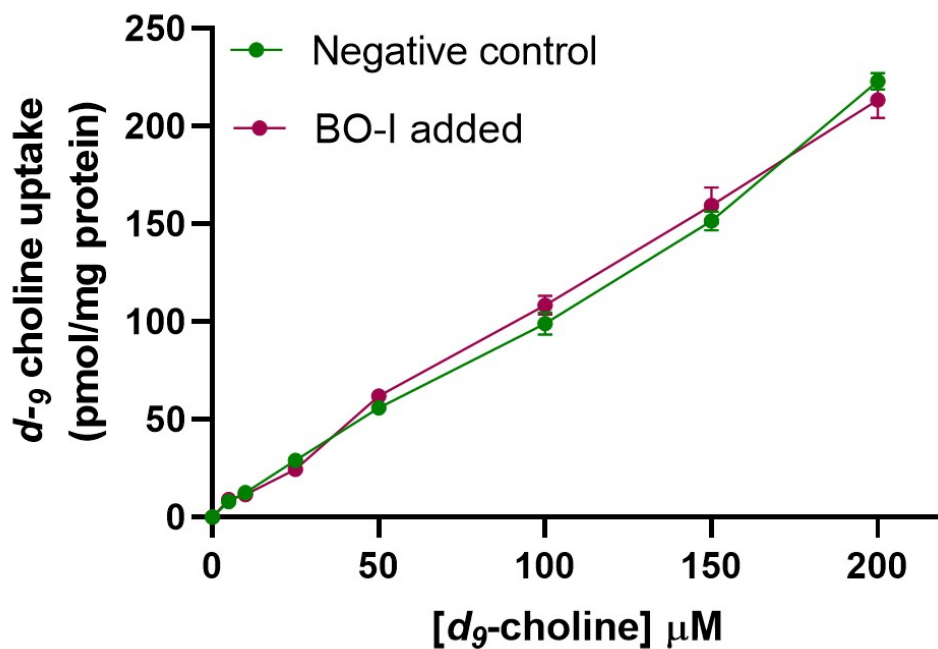


**Fig. S1.** The effect of BO-I (50  $\mu\text{M}$ ) on choline uptake in *Escherichia coli* (*E. coli*) MS 200-1 at various added concentrations of  $d_9$ -choline. Bacterial uptake studies were performed as previously reported.<sup>1</sup>

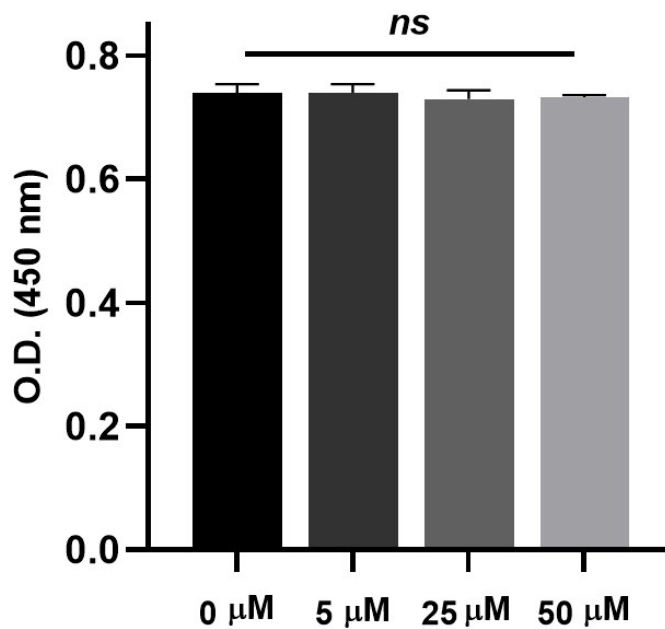


**Fig. S2.** Evaluation of alcohol dehydrogenase activity using alcohol dehydrogenase activity kit (ab102533) in the absence and presence of different concentrations of BO-I. Error bars represent standard deviation ( $n = 3$ ), *ns* denotes non-significant difference.

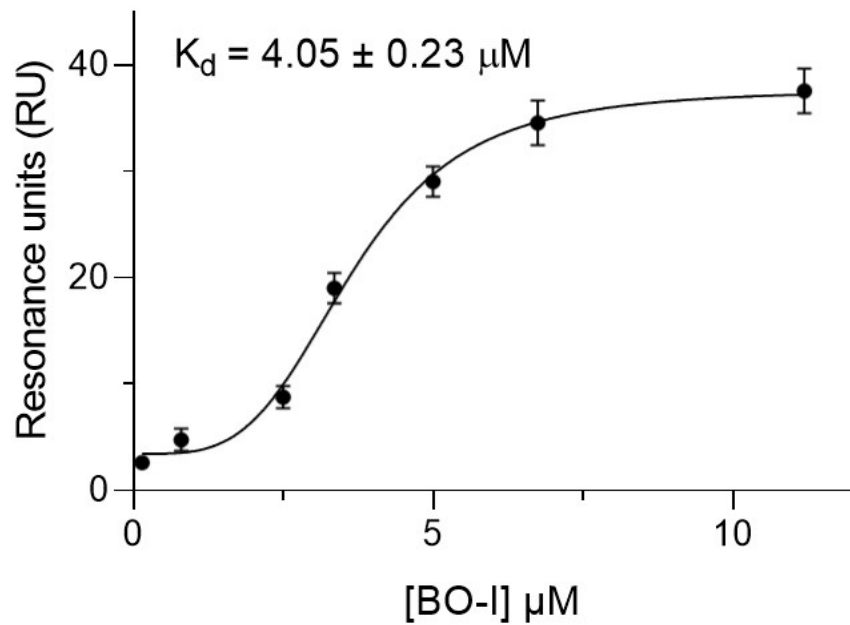


**Fig. S3.** SPR binding curve for BO-I to CutC. Error bars represent standard deviation ( $n = 3$ ).

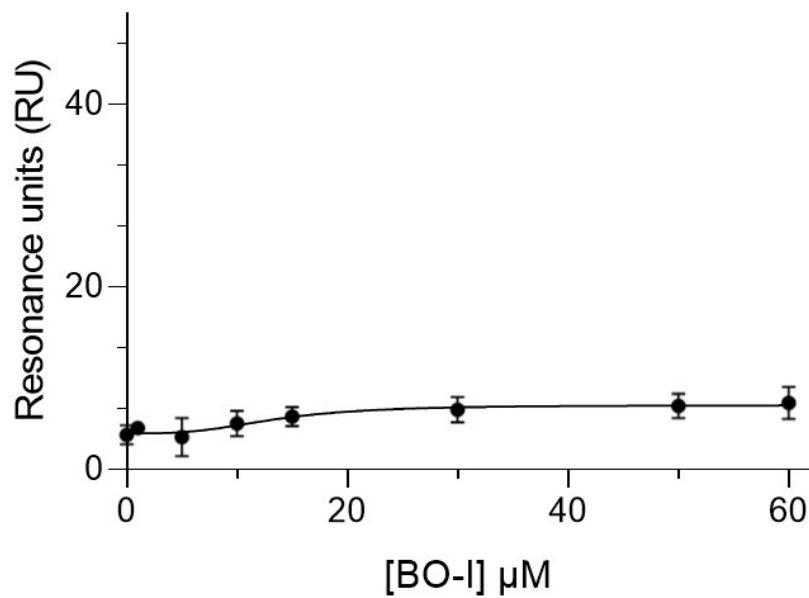


**Fig. S4.** SPR binding curve for BO-I to CutD. Error bars represent standard deviation ( $n = 3$ ).

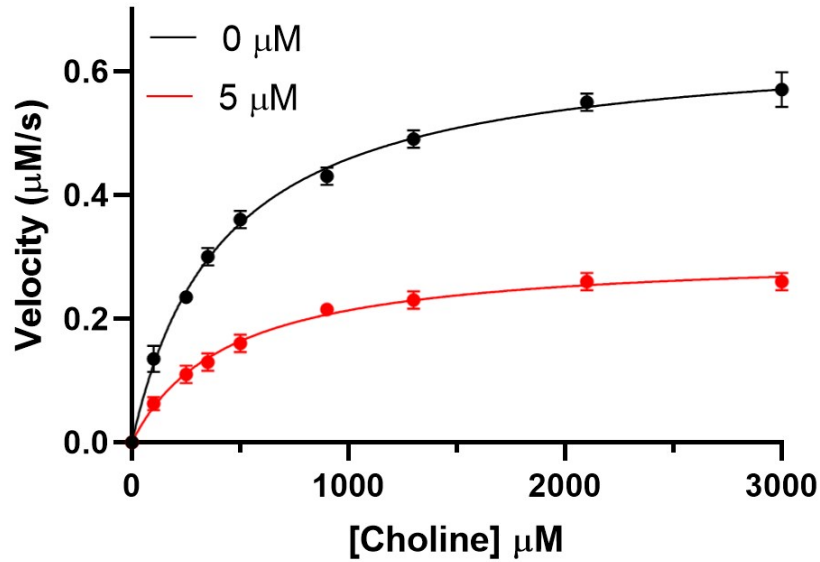


**Fig. S5.** Michaelis–Menten plot of the reaction velocity against various concentrations of choline in the absence and presence of BO-I (5  $\mu\text{M}$ ). Error bars represent standard deviation ( $n = 3$ ).

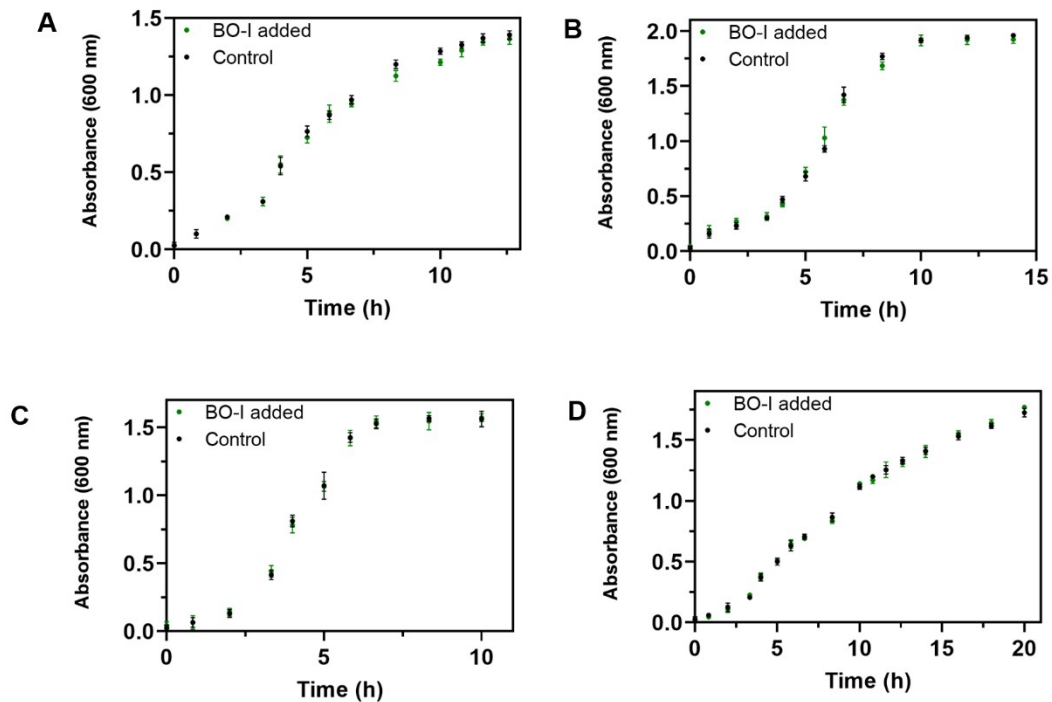


**Fig. S6.** Bacterial growth kinetics based on absorbance measurements in the absence and presence of BO-I (25  $\mu\text{M}$ ) for (A) *E. coli* MS 200-1 (B) *Klebsiella sp.* MS 92-3 (C) *Proteus mirabilis*, and (D) *Clostridium sporogenes*. Error bars represent standard deviation ( $n = 3$ ).

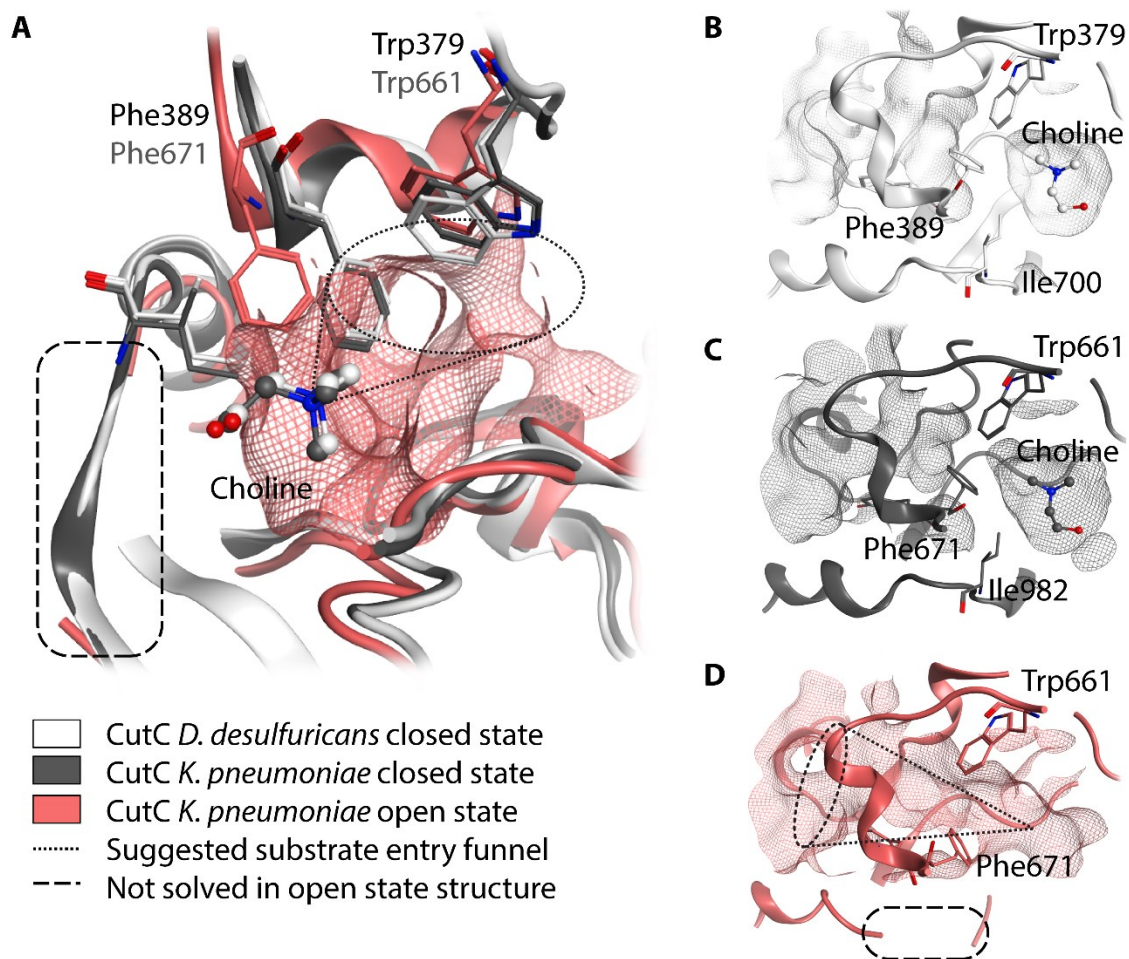


**Fig. S7.** Suggested substrate entry funnel of CutC from *D. desulfuricans* and *K. pneumoniae*. In the X-ray structures of the closed choline-bound state the suggested substrate entry funnel is closed by Phe389/671 which is potentially hold in place by Ile700/982 (**A-C**; PDB-IDs: 5FAU, 5A0Z). In the X-ray structure of the open choline-free state Phe389/671 moved aside to open the putative entry channel (**A, D**; PDB-ID: 5A0U). The Ile982-carrying loop is not resolved in the open state.

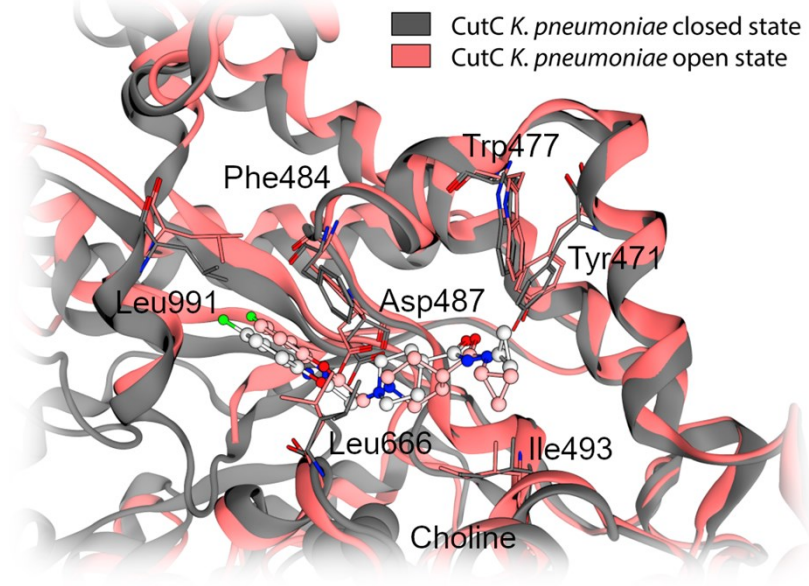


**Fig. S8.** Suggested binding mode of BO-I to the putative substrate entry funnel of CutC from *K. pneumoniae* in the open and closed state.



## References

- 1 Z. Wang, A. B. Roberts, J. A. Buffa, B. S. Levison, W. Zhu, E. Org, X. Gu, Y. Huang, M. Zamanian-Daryoush, M. K. Culley, A. J. DiDonato, X. Fu, J. E. Hazen, D. Krajcik, J. A. DiDonato, A. J. Lulis, S. L. Hazen, *Cell* 2015, **163**, 1585-1595.